و , [5] و , كمه و فح و , [2-4]
و و ئى [6] و :1)
حمس [7-9] ;2) [10-11]
, سج و , [12] طمه
, [13-14]
(microbially induced calcite precipitation, MICP) يم ,
طمه و [15] ئؤ MICP و ,
pH , (CO_2 HCO_3^- CO_3^{2-}) , طمه [16] ,MICP
و طى ضمه [17-19]
[20] MICP و نج ئى و , MICP ئؤ و
[21] MICP و , 0.25 mol/L مخج 0.50 mol/L ,
0.13 MPa مخج 1.36 MPa [22] MICP و ,
2.0 mol/L , ,MICP و و [23]
و MICP , و 14% , , و
مخج
MICP و , MICP و و
, ئؤ , MICP و
, و , و
, يم - و

1

1.1

1.1.1 و

و , ئى 3 ~ 5 m و
(GB/T 50123—2019) نج , 1

1 Ǎ و

Table 1 Physical properties of Malan loess

Physical property	Value
Relative density	2.55
Liquid limit/%	28.26
Plasticity limit/%	10.76
Plasticity index/%	18.19
Maximum dry unit weight/($kN \cdot m^{-3}$)	15.3
Optimum water content (mass fraction)/%	15.1

1.1.2

, (ATCC 11859)
ئؤ 25 , 20 g/L 15 g/L 5 g/L 5 g/L
مه نج pH 7.3 مه نج ئؤ 121 1 MPa 30 min,
مه 1 100 مه نج , مه نج 30 160 r/min مه
مه 24 h (OD_{600}) 1.9 ± 0.1, (34.2 ± 0.5) mmol/min
600 nm , [24-25]
ئؤ $CaCl_2$ [26] , MICP
و , 0.2 0.4 0.6 0.8 1.0 mol/L

1.2 و ̈Ạ

و 2 mm , ئؤ 60 48 h و 17% ,

(0 mol/L) ئؤ 2.0 ±0.1 1 1 و ,
67 r/min 240 s
, (38.1 mm × 76.2 mm) , ǻ = 25 N, 200 g شج
و , و = 5, ` = 30 cm, ، = 20/
, ئؤ , 25 95% طمم 3 7 14 d

1.3

[27-28]

, و ه 1

,

,

0.8 cm × 0.8 cm ,

,

0.5 s

ئؤ , 30 s

, ,

, 90 s ,

(1)

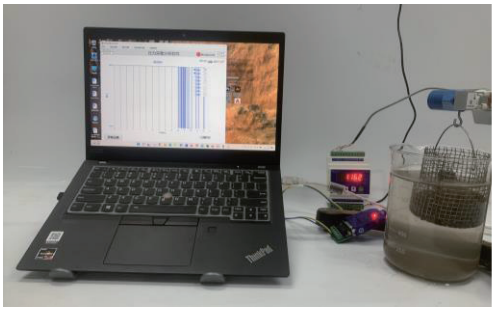

ه 1

Fig. 1 Self-designed disintegration instrument

$$= \frac{\ddot{\alpha}_0 - \ddot{\alpha}}{{}_0} \times 100 \qquad (1)$$

: $\ddot{\alpha}_0$ $\ddot{\alpha}$, ثي g; $_0$

,200 g

, , , و

$\ddot{\alpha}_{max}$, (1) $\ddot{\alpha}_0$

$\ddot{\alpha}_{max}$, و , $_0$ و $_0 + \ddot{\alpha}_{max} - \ddot{\alpha}_0 (\ddot{\alpha}_{max} - \ddot{\alpha}_0$

) , (2)

$$= \frac{\ddot{\alpha}_{max} - \ddot{\alpha}}{{}_0 + \ddot{\alpha}_{max} - \ddot{\alpha}_0} \times 100 \qquad (2)$$

2 ٌ

2.1 ٌ

و [29] , , و

و , و , ئؤ ,

, ,

, ئؤ , و , و

, و [30] ; و ئؤ و

, , , [31]

, ئؤ , نج ئؤ , ,

نج , و [5,32]

و شج , و , و , سج و

و , , و ,

, , ,

ه 2 - ه 2 , MICP و

, ئؤ ( ) مخ
مخ , ئؤ ه 2 و و
و , ه 2(a) , ئؤ 3 d , و
, ئؤ 0.6 mol/L , 0.6 mol/L
ه 2(b) , ئؤ 7 d , 0.8 1.0 mol/L ئؤ
, 0.2 0.6 mol/L ه 2(c) , ئؤ 14 d
,MICP و مخ , و 3 ~ 6 0.6 mol/L
, , 13 28 min, و
1 12 min, 0.6 mol/L , مخ
حس مخ , ضم [23] ,
, طمه , [33]

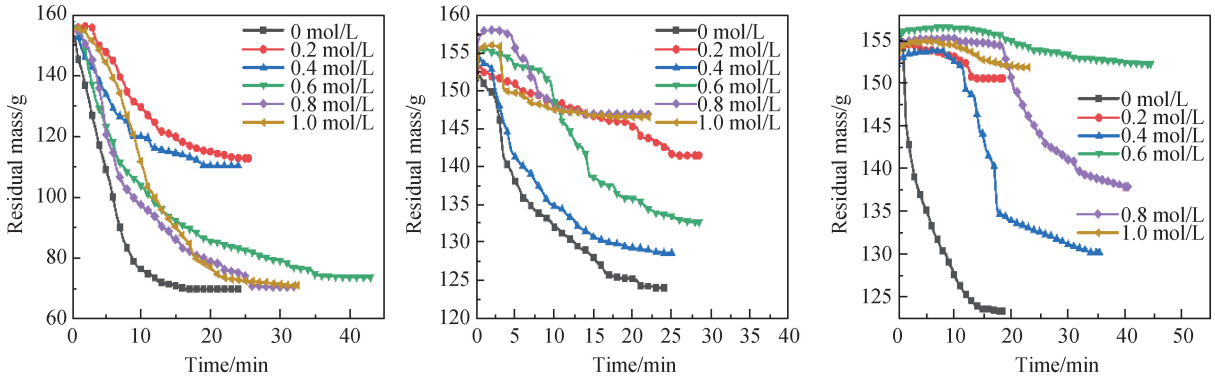

(a) 3 d (b) 7 d (c) 14 d

ه 2 -

Fig. 2 Residual mass-time curves during disintegration under different curing ages

2.2 ẽ ĩ

ه 3 و , ه ثي 0 0.2 0.4 0.6 0.8
1.0 mol/L ه 3 MICP ثي , ئؤ 14 d
مخ ,MICP و مخ

(a) 3 d (b) 7 d (c) 14 d

ه 3 و

Fig. 3 Loess disintegration results under different curing ages

ه 3(a) , 3 d , , 0.2 0.4 mol/L
, ه 3(b) ه 3(c) , 7 14 d ,
, 0.2 0.6 0.8 1.0 mol/L,
مخ , 0.6 mol/L مخ ئؤ 14 d ,

[33-34] , ,

مخ , Zheng [35]

2.3

ه 4 (2) - ه 4 ,MICP

ثي ه 4(a) , 3 d ,MICP

ه 4(b) , مخ 7 d ,MICP ثي

ه 4(c) : 14 d ,MICP 28% ~80% , ئؤ 0.2

0.6 1.0 mol/ ثي 0.02% ; 0.16% , ئؤ 0.6 mol/L

, , ئؤ 14 d ,

0.6 mol/L MICP و [27]

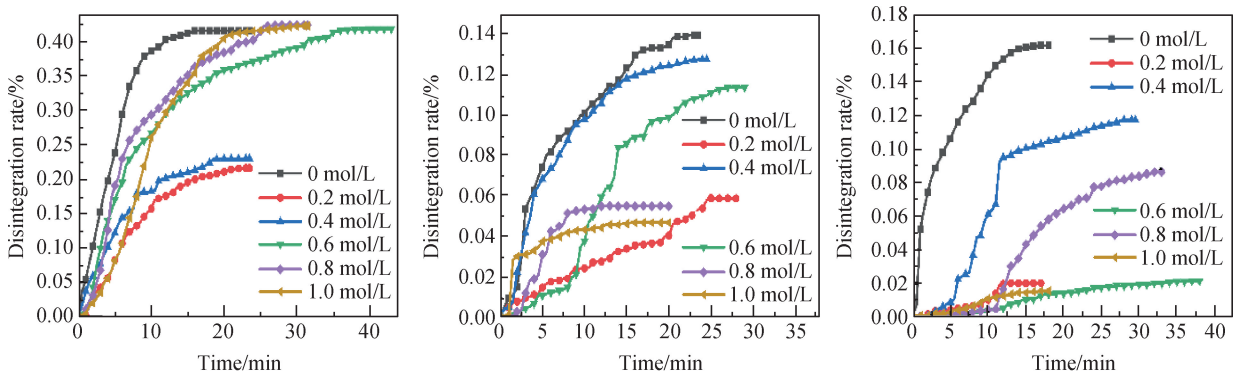

(a) 3 d (b) 7 d (c) 14 d

ه 4 -

Fig. 4 Disintegration rate-time curves during disintegration under different curing ages

2.4 Ó Ą̈

و نج [29,36] , و نج ثي

[37] و , و ئؤ ,

Þ و ((3)) [38]

Þ = (- ᵘ̈ₐ) + Ü̈(ᵘ̈ₐ - ᵘ̈ᵥ) (3)

: ;ᵘ̈ₐ ;Ü̈ , ;ᵘ̈ᵥ ,(ᵘ̈ₐ - ᵘ̈ᵥ) نج

ئؤ سج , , =0 , ,

, ᵘ̈ₐ = ₐ , , ئؤ

, نج ᵘ̈Þₐ , Þ (4)

Þ = (- ₐ - ᵘ̈Þₐ) + Ü̈(ₐ - ᵘ̈ᵥ) (4)

و [32] , , و مخ

, Ü̈ , ᵘ̈ᵥ ,

مخ , نج , Ü̈(ₐ - ᵘ̈ᵥ) - ₐ ,Ü̈

و , ᵘ̈Þₐ مخ , (5)

- ᵘ̈Þₐ = (5)

: ; و

ئؤ d گd ,

$$= \frac{d^2 گ}{d^2} \quad (6)$$

(6) (5)

$$- ᵘ̈Þₐ = \frac{d^2 گ}{d^2} \quad (7)$$

و , و , و

dگ , (8)

$$\text{ـ} = \text{ـ}_{a}\text{گ}^{3} = \text{س} \tag{8}$$

: ; ; = گ³ ; ; س ;

(8) (7)

$$-\frac{\text{س}}{\text{گ}^{3}} = \frac{d^{2}\text{گ}}{d^{2}} \tag{9}$$

ئۇ , ثي , و س

, - س , ڭ

$$\frac{\text{ڭ}}{\text{گ}^{3}} = \frac{d^{2}\text{گ}}{d^{2}} \tag{10}$$

$$\text{گ} = \sqrt{\text{ۋ}_{1}(2^{2} - 4\text{ۋ}_{2} + 2\text{ۋ}_{2}^{2}) + \frac{\text{ڭ}}{2\text{ۋ}_{1}}} \tag{11}$$

و ,

$$\text{ئا}_{max} - \text{ئا} = \text{ئىن} \tag{12}$$

$$_{0} + \text{ئا}_{max} - \text{ئا}_{0} = \tag{13}$$

: ن ;

(12) (13) (2)

$$= \frac{\text{ئا}_{max} -}{_{0} + \text{ئا}_{max} - \text{ئا}_{0}} \times 100 = \frac{\text{ن}}{} \sqrt{\text{ۋ}_{1}(2^{2} - 4\text{ۋ}_{2} + 2\text{ۋ}_{2}^{2}) + \frac{\text{ڭ}}{2\text{ۋ}_{1}}} \tag{14}$$

: ۋ1 ۋ2 ; ن

,

-

(ه 5)

0.6 mol/L و

: ۋ1 = 3.15, ۋ2 = 6.18 × 10⁻⁷,

ڭ = - 1.19 × 10⁻¹³, $^{2}_{adjusted}$ = 0.91; ۋ1 = - 36.13, ۋ2 =

1.11 × 10⁻⁵, ڭ = - 5.17 × 10⁻⁷, $^{2}_{adjusted}$ = 0.95, -

ئۇ ثي 0.90

ئۇ 14 d 0.6 mol/L

, MICP و ,

2 , 0.14% 0.02%, 2.3

, MICP ڭ , MICP

, , و ,

و

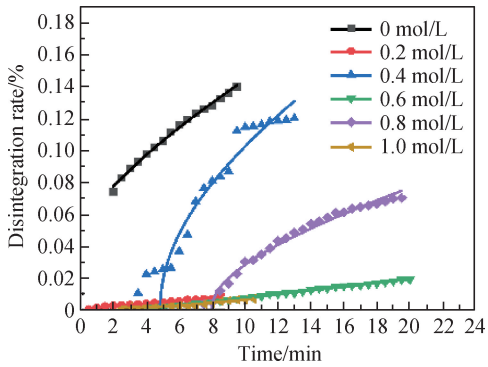

ه 5 14 d و

Fig. 5 Fitting curves of disintegration rate of loess sample curing 14 d

3

1) , MICP متج متج ئۇ

14 d MICP و متج , و 3 ~ 6 0.6 mol/L

, 13 28 min, و 1 12 min,

متج حمس متج , ضم , ,

, طمه , ,

2) ئۇ 14 d , مۇنچ , 0.6 mol/L مۇنچ

, ,

مۇنچ

3) MICP ثي , 14 d ,MICP 28% ~80% ,

ئۇ 0.2 0.6 1.0 mol/L ثي 0.02% , 0.16%

ئۇ 14 d , 0.6 mol/L MICP و

4) و يم 0.90 ,

MICP

و , ,

د

[1] LIU X J, PAN C F, YU J, et al. Study on micro-characteristics of microbe-induced calcium carbonate solidified loess[J]. Crystals, 2021, 11 (12): 1492.

[2] . ئى و و [J]. و , 2022(5): 55-57.
HUANG Q H. Review on the effects of land use on soil erosion [J]. Technology of Soil and Water Conservation, 2022(5): 55-57 (in Chinese).

[3] . فج [J]. ئى , 2020, 28(2): 360-374.
XU Q. Understanding the landslide monitoring and early warning: consideration to practical issues[J]. Journal of Engineering Geology, 2020, 28 (2): 360-374 (in Chinese).

[4] . نجئى و [J]. , 2022(7): 70-71+77.
ZHAO X D. Study on treatment method of collapsible loess foundation [J]. Sichuan Cement, 2022(7): 70-71+77 (in Chinese).

[5] , , . و [J]. , 2009, 28(s1): 3207-3213.
LI X A, HUANG R Q, PENG J B. Experimental research on disintegration of loess[J]. Chinese Journal of Rock Mechanics and Engineering, 2009, 28(s1): 3207-3213 (in Chinese).

[6] , , , . و شج [J]. , 2014, 31(10): 146-150+155.
GAO J W, YU H M, QIAN Y Z, et al. Experimental study on disintegration characteristics of remolded loess[J]. Journal of Yangtze River Scientific Research Institute, 2014, 31(10): 146-150+155 (in Chinese).

[7] . و [J]. , 2022(12): 219-221.
LI C J. Road construction technology and innovation practice for special soil section[J]. Construction & Design for Engineering, 2022(12): 219-221 (in Chinese).

[8] , , , . نجئى و [J]. , 2021, 41(6): 1366-1381.
WANG Q, LIU Z Z, WANG L M, et al. Review on seismic reinforcement of loess foundation[J]. Journal of Disaster Prevention and Mitigation Engineering, 2021, 41(6): 1366-1381 (in Chinese).

[9] . نجئى و [J]. , 2022(1): 1-5+34.
BAI X H. Collapsible loess and new technology of foundation treatment[J]. Shanxi Science & Technology of Transportation, 2022(1): 1-5+34 (in Chinese).

[10] , , , . [J]. ئى , 2006, 2(3): 510-516.
ZHOU J, ZHANG S F, JIA M C, et al. Theoretic research situation and latest technical progress of dynamic consolidation method[J]. Chinese Journal of Underground Space and Engineering, 2006, 2(3): 510-516 (in Chinese).

[11] FENG S J, DU F L, SHI Z M, et al. Field study on the reinforcement of collapsible loess using dynamic compaction[J]. Engineering Geology, 2015, 185: 105-115.

[12] WU W B, YANG Z J, LIU X, et al. Horizontal dynamic response of pile in unsaturated soil considering its construction disturbance effect[J]. Ocean Engineering, 2022, 245: 110483.

[13] , , . LD و و [J]. , 2003, 22(s2): 2888-2893.
WANG S J, HAN W F, WANG Y M. Testing study on loess consolidated by LD serial rock-soil cemedin[J]. Chinese Journal of Rock Mechanics and Engineering, 2003, 22(s2): 2888-2893 (in Chinese).

[14] , , . و [J]. , 2001, 21(1): 15-18.

PENG B, LI W Y, DAI J L. Research on liquid stabilizer reinforced soil[J]. Journal of Xi'an Highway University, 2001, 21(1): 15-18 (in Chinese).

[15] , , , . و MICP [J]. ئی , 2020, 16(1): 295-302.
JIN G X, ZHANG J X, XU K, et al. Influence of particle gradation on grouting effect of microbial induced calcite precipitated of residual soil impact assessment[J]. Chinese Journal of Underground Space and Engineering, 2020, 16(1): 295-302 (in Chinese).

[16] , , . و [J]. , 2022, 41(3): 969-975.
KONG D C, SUN Z G, JIA F F. Microbial induced calcium carbonate precipitation technique for improving collapsibility of loess[J]. Bulletin of the Chinese Ceramic Society, 2022, 41(3): 969-975 (in Chinese).

[17] DYSON G J, RANDOLPH M F. Monotonic lateral loading of piles in calcareous sand[J]. Journal of Geotechnical and Geoenvironmental Engineering, 2001, 127(4): 346-352.

[18] , , , . نج مخ و [J]. , 2022, 41(2): 479-487.
FAN Y D, WANG Y Z, XU S S, et al. Self-healing performance of cracks in recycled concrete based on coarse aggregates enhanced by MICP of mixed cultures of bacteria[J]. Bulletin of the Chinese Ceramic Society, 2022, 41(2): 479-487 (in Chinese).

[19] , , , . [J]. , 2018, 37(5): 1509-1514.
TONG T Z, MIAO L C, SUN X H, et al. Microbially-induced carbonate precipitation in low temperature[J]. Bulletin of the Chinese Ceramic Society, 2018, 37(5): 1509-1514 (in Chinese).

[20] , , , . نج ئی و [J]. و , 2013, 35(8): 1486-1495.
CHENG X H, MA Q, YANG Z, et al. Dynamic response of liquefiable sand foundation improved by bio-grouting[J]. Chinese Journal of Geotechnical Engineering, 2013, 35(8): 1486-1495 (in Chinese).

[21] . (MICP) و [D]. : ئی ( ), 2014.
ZHAO Q. Experimental study on soil improvement using microbial induced calcite precipitation (MICP)[D]. Beijing: China University of Geosciences, 2014 (in Chinese).

[22] . MICP و [D]. : , 2020.
MA Y R. Experimental study on mechanical properties and mechanism of loess reinforced by MICP[D]. Taiyuan: Taiyuan University of Technology, 2020 (in Chinese).

[23] . و MICP [D]. : , 2020.
FAN J Y. Study on MICP solidification mechanism and mechanical properties of loess[D]. Xi'an: Xi'an University of Architecture and Technology, 2020 (in Chinese).

[24] WHIFFIN V S, VAN PAASSEN L A, HARKES M P. Microbial carbonate precipitation as a soil improvement technique[J]. Geomicrobiology Journal, 2007, 24(5): 417-423.

[25] HARKES M P, VAN PAASSEN L A, BOOSTER J L, et al. Fixation and distribution of bacterial activity in sand to induce carbonate precipitation for ground reinforcement[J]. Ecological Engineering, 2010, 36(2): 112-117.

[26] , , , . بخ [J]. و , 2019, 40(4): 1291-1298.
LI C, WANG S, WANG Y X, et al. Field experimental study on stability of bio-mineralization crust in the desert[J]. Rock and Soil Mechanics, 2019, 40(4): 1291-1298 (in Chinese).

[27] ZHANG H N, JIA C Q, WANG G H, et al. Physical-mechanical properties of microbially induced calcite precipitation-treated loess and treatment mechanism[J]. Journal of Mountain Science, 2022, 19(10): 2952-2967.

[28] LIANG S H, XIAO X L, FANG C X, et al. Experimental study on the mechanical properties and disintegration resistance of microbially solidified granite residual soil[J]. Crystals, 2022, 12(2): 132.

[29] LI X, WANG L, YAN Y L, et al. Experimental study on the disintegration of loess in the Loess Plateau of China[J]. Bulletin of Engineering Geology and the Environment, 2019, 78(7): 4907-4918.

[30] , . طه و [J]. , 2021(3): 6-12.
FAN N N, LI Y R. Preliminary research on the disintegration of Malan loess with roots in different water environments[J]. China Rural Water and Hydropower, 2021(3): 6-12 (in Chinese).

[31] . [J]. ( ), 2013, 33(5): 1-6.
LEI S Y. Theoretical analysis of effects of capillary water on strength of slight wet silt sand[J]. Journal of Chang'an University (Natural Science Edition), 2013, 33(5): 1-6 (in Chinese).

[32] , , , . و MICP [J]. , 2021, 37(22): 127-135.
LI A J, XU C, LI X, et al. Experimental investigation on disintegration characteristics and MICP reinforcement of unsaturated sandy clayey purple soil[J]. Transactions of the Chinese Society of Agricultural Engineering, 2021, 37(22): 127-135 (in Chinese).

63(3/4): 239-240.

[82] RUH R, GARRETT H J. Nonstoichiometry of ZrO_2 and its relation to tetragonal-cubic inversion in ZrO_2[J]. Journal of the American Ceramic Society, 1967, 50(5): 257-261.

[83] RUH R. Proposed phase diagram for the system ZrO_2[J]. Journal of the American Ceramic Society, 1970: 360.

[84] RAMESH S, SARA LEE K Y, TAN C Y. A review on the hydrothermal ageing behaviour of Y-TZP ceramics[J]. Ceramics International, 2018, 44(17): 20620-20634.

[85] ZHANG F, VANMEENSEL K, BATUK M, et al. Highly-translucent, strong and aging-resistant 3Y-TZP ceramics for dental restoration by grain boundary segregation[J]. Acta Biomaterialia, 2015, 16: 215-222.

[86] NOGIWA-VALDEZ A A, RAINFORTH W M, ZENG P, et al. Deceleration of hydrothermal degradation of 3Y-TZP by alumina and lanthana co-doping[J]. Acta Biomaterialia, 2013, 9(4): 6226-6235.

[87] ZHANG F, VANMEENSEL K, INOKOSHI M, et al. Critical influence of alumina content on the low temperature degradation of 2 ~ 3 mol% yttria-stabilized TZP for dental restorations[J]. Journal of the European Ceramic Society, 2015, 35(2): 741-750.

[88] MATSUI K, NAKAMURA K, KUMAMOTO A, et al. Low-temperature degradation in yttria-stabilized tetragonal zirconia polycrystal doped with small amounts of alumina: effect of grain-boundary energy[J]. Journal of the European Ceramic Society, 2016, 36(1): 155-162.

[89] TREDICI I G, SEBASTIANI M, MASSIMI F, et al. Low temperature degradation resistant nanostructured yttria-stabilized zirconia for dental applications[J]. Ceramics International, 2016, 42(7): 8190-8197.

[90] ARAGÓN-DUARTE M C, NEVAREZ-RASCÓN A, ESPARZA-PONCE H E, et al. Nanomechanical properties of zirconia- yttria and alumina zirconia- yttria biomedical ceramics, subjected to low temperature aging[J]. Ceramics International, 2017, 43(5): 3931-3939.

[91] HARADA A, SHISHIDO S, BARKARMO S, et al. Mechanical and microstructural properties of ultra-translucent dental zirconia ceramic stabilized with 5 mol% yttria[J]. Journal of the Mechanical Behavior of Biomedical Materials, 2020, 111: 103974.

[92] ZHANG F, VAN MEERBEEK B, VLEUGELS J. Importance of tetragonal phase in high-translucent partially stabilized zirconia for dental restorations[J]. Dental Materials, 2020, 36(4): 491-500.

[93] DOS SANTOS C, ROSA G O, QUINTINO M N, et al. Effect of surface finishing and thickness on the translucency of zirconia dental ceramics[J]. Ceramics International, 2020, 46(6): 7748-7755.

[94] HAYAISHI Y, MIKI H, YOSHIKAWA H, et al. Phase transformation of a new generation yttria-stabilized zirconia femoral head after total hip arthroplasty[J]. Modern Rheumatology, 2008, 18(6): 647-650.

[95] PRADO P H C O, MONTEIRO J B, CAMPOS T M B, et al. Degradation kinetics of high-translucency dental zirconias: mechanical properties and in-depth analysis of phase transformation[J]. Journal of the Mechanical Behavior of Biomedical Materials, 2020, 102: 103482.

(681)

[33] ZHAO Q, LI L, LI C, et al. Factors affecting improvement of engineering properties of MICP-treated soil catalyzed by bacteria and urease[J]. Journal of Materials in Civil Engineering, 2014, 26(12): 04014094.

[34] SON Y, MIN J, JANG I, et al. Development of a novel compressed tablet-based bacterial agent for self-healing cementitious material[J]. Cement and Concrete Composites, 2022, 129: 104514.

[35] ZHENG T W, SU Y L, ZHANG X, et al. Effect and mechanism of encapsulation-based spores on self-healing concrete at different curing ages[J]. ACS Applied Materials & Interfaces, 2020, 12(47): 52415-52432.

[36] , . [J]. , 2007, 29(10): 1591-1592.
LU J, CHENG B. Research on soil-water characteristic curve of unsaturated loess[J]. Chinese Journal of Geotechnical Engineering, 2007, 29(10): 1591-1592 (in Chinese).

[37] , , . [J]. , 2011, 32(11): 3258-3262.
WANG J E, XIANG W, BI R N. Experimental study of influence of matric suction on disintegration of unsaturated remolded loess[J]. Rock and Soil Mechanics, 2011, 32(11): 3258-3262 (in Chinese).

[38] BISHOP A. The principle of effective stress[J]. Teknisk Ukeblad, 1959, 39: 859-863.